

## Resonant tunneling of photons in layered optical nanostructures (metamaterials)

© M.V. Davidovich

Saratov National Research State University, Saratov, Russia  
e-mail: tdavidovichmv@info.sgu.ru

Received December 16, 2022

Revised December 16, 2022

Accepted December 16, 2022

The conditions of resonant (almost complete) tunneling of photons (plane monochromatic electromagnetic waves) through layered dielectric and metal-dielectric structures are considered. Resonant tunneling occurs at frequencies at which the resonance conditions for the corresponding structures of open resonators are met. For metal-dielectric structures, the possibility of tunneling in the optical range with a strong barrier in the IR range is shown, which can be used to control the transmission of window panes.

**Keywords:** dielectric permittivity, homogenization, resonant tunneling, plasmons, metal nanoparticles, window panes.

DOI: 10.21883/TP.2023.04.55937.275-22

### Introduction

Resonant tunneling (RT) is a quantum wave effect of total resonant transmission of particles through structures that have two or more strongly reflecting elements, between which particles move almost freely [1–7]. In this case, in the vicinity of the reflecting element, the waves are evanescent. In fact, RT means such interference of reflected waves, in which the total reflection coefficient  $R$  equals zero. When modeling RT, 1D structures are considered and the momentum of particles in the direction of motion is taken into account, i.e., one-dimensional problems are solved. RT began to be used over 50 years ago in solid-state resonant tunneling diodes and resonant tunneling transistors [6–21], in which a quantum heterostructure was created that forms two or more potential barriers for tunneling electrons, separated by a region or several regions, which are sometimes referred to as quantum wells. Such a heterostructure is made from nanoscale layers of wide-gap and narrow-gap semiconductor, e.g.,  $\text{Al}_x\text{Ga}_{1-x}\text{As}$  and GaAs with ohmic contacts on the GaAs cathode and anode. The energy bottom of the well must be lower than the energy of incident electrons, and in this case, the formation of metastable levels in the well is possible. The quantum potential configuration can be controlled by doping. In solid-state structures, charge carriers are understood as quasi-particles with a certain effective mass  $\mu$ , i.e. holes can also be considered, and the simplest form of such a quantum potential  $V(z)$  can have two rectangular barriers counted from the zero level, separated by a region with zero potential. Since particles with mass  $\mu$  have wave properties, and their motion obeys the Schrödinger equation (SE) with wave function  $\psi(z)$ , they can be assigned momentum  $p = \hbar k$  and wavenumber  $k = \sqrt{2\mu(E - V(z))}/\hbar = i\kappa$ , and the motion can be described by wave admittance

$\eta(z) = -i\psi'(z)/\psi(z) = k$ , since the wave function and its derivative must be continuous everywhere. The condition  $R = 0$  in the case of two identical rectangular barriers leads to the equation [22]:

$$\tan(kt_w) \tanh(\kappa t_B) = -\frac{2i\tilde{\eta}}{1 + \tilde{\eta}^2} = \frac{\sqrt{V/E - 1}}{1 - (1/2)V/E}. \quad (1)$$

At  $V/E > 1$ , this complex transcendent equation can have complex roots, corresponding to the RT energy levels. Here  $t_B$  denotes the barrier (depleted region) size,  $t_w$  is the well size,  $V$  is the rectangular barrier height, and  $\tilde{\eta} = \eta(V)/\eta(0)$  is the ratio of wave admittances. Hereinafter the tilde denotes normalized quantities. In a symmetric structure, there is a similar back current (flux) of electrons. Asymmetry arises upon the application of anode voltage. The RT is also possible for the motion through two potential wells ( $V < 0$ ) [20].

There is a direct analogy between the stationary SE and the Helmholtz wave equation in electrodynamics, i.e., between tunneling of electrons and photons [22–25]. Namely, the propagation of a plane wave through the space with permittivity  $\varepsilon(z)$  is equivalent to the motion of an electron in a potential field  $V$ , if we take into account the relation  $k_0^2 \varepsilon(z) = 2m_e E(1 - V(z)/E)/\hbar^2$ , from which we conclude that there is a correspondence  $\varepsilon(z) = 1 - V(z)/E$  to the motion of a plane electromagnetic wave in the direction of the  $z$ -axis. Therefore, the absence of the potential corresponds to the motion of a photon in vacuum ( $\varepsilon = 1$ ), the condition  $V(z)/E > 1$  (tunneling) means  $\varepsilon(z) < 0$ , which corresponds to the photon motion through a collisionless plasma, and the condition  $V(z)/E < 1$  corresponds to the over-barrier ( $V > 0$ ) and over-well ( $V < 0$ ) motion. These two cases correspond to conditions  $0 < \varepsilon(z) < 1$  and  $\varepsilon(z) > 1$ , (plasma above the plasma frequency) and (dielectric). The condition  $\varepsilon \approx 1$  can be fulfilled in a low-dissipation plasma; in electrodynamics, it corresponds to

waves in ENZ (epsilon-near-zero) media [26]. In quantum mechanics  $V(z) = E$  corresponds to a singular point. It is important to note that the RT can be total in the absence of dissipation, which is so in quantum mechanics due to the conservation of the number of particles. In electrodynamics, this requires neglecting the absorption of photons. It should be also kept in mind that a photon with energy  $\omega\hbar$  in a medium is a quasiparticle (quasiphoton) with a different momentum; in particular, in a plasma an imaginary momentum should be attributed to it. The strongly expressed resonance structure (RS) for a photon arises when there are two sharp plasma layers, separated by a vacuum or dielectric gap. For the electron, this is an analog of the potential with two humps separated by a potential well. Another resonant structure can have the form of two dielectric plates with high permittivity separated by a vacuum gap or a low-permittivity layer. In optics, both structures are open resonators, whose radiative Q factors are the higher, the higher is the reflection from the layers (plates). However, in the second case one should speak of resonant transmission rather than of resonant tunneling. The reflection depends on the thickness of the layers and on the difference of the permittivity from one. That is why under the condition  $0 < \varepsilon < 1$  plasma layers are low efficient for the formation of sharp resonances. In cold plasma, it is difficult to produce layers with sharp boundaries. A possible exception can be the case of placing plasma in glass vessels with thin planar walls. It is easier to implement plasma using metallic or semiconductor layers; in this case, the layers can be made to have the thickness from a few nanometers to rather high values. A radical reduction of losses is possible through using cryogenic temperatures. Making RSs with high-permittivity layers is limited by the choice of materials, the anisotropy of their permittivity, and the dissipation. For example, semiconductor materials with the permittivity above 10, as a rule, have high losses. For a dielectric layer  $\tilde{\eta} = \sqrt{\varepsilon}$ , and for a plasma layer  $\tilde{\eta} = i\sqrt{|\varepsilon|}$ , therefore, Eq. (1) is valid in these cases, too. However, in optics structures of two layers separated a dielectric payer are more practical. This changes the wave admittances ratio; the left-hand side of Eq. (1) should be taken in the form  $\tan(k_0 t_W \sqrt{\varepsilon_W}) \tanh(k_0 t_B \sqrt{|\varepsilon_B|})$ . Here  $\varepsilon_B < 0$  corresponds to the permittivity of plasma. For  $\varepsilon_B > \varepsilon_W$  we should make the replacement  $\tanh(k_0 t_B \sqrt{|\varepsilon_B|}) \rightarrow -i \tan(k_0 t_B \sqrt{\varepsilon_B})$ .

## 1. Multilayered tunneling RSs with metal-dielectric layers

For tunneling photons it is reasonable to consider diffraction of a plane electromagnetic wave  $\mathbf{E} = \mathbf{e}_0 E_0 \exp(-ik_0 z)$ ,  $\mathbf{H} = \mathbf{z}_0 \mathbf{e} \sqrt{\varepsilon_0/\mu_0} E_0 \exp(-ik_0 z)$ , by a multilayer dissipation-free RS,  $\mathbf{e}_0 = \mathbf{x}_0$ . For a wave incident at angle in the plane  $\theta$  ( $x, z$ ) one should use the dependences  $\exp(-ik_z z - ik_x x)$ ,  $k_z = \sqrt{k_0^2 - k_x^2}$ , and the polarization direction  $\mathbf{e}_0 = \mathbf{x}_0 \cos(\varphi) + \mathbf{z}_0 \sin(\varphi)$  or  $\mathbf{e}_0 = (\mathbf{x}_0 k_z + \mathbf{z}_0 k_x)/k_0$ , since in this case an  $E$ -wave

is considered. For this wave the normalized medium admittance is  $\tilde{y}_e = \sqrt{\mu_0/\varepsilon_0} H_y/E_x = k_0 \varepsilon/k_z$ . For the other polarization  $\tilde{y}_h = k_z/k_0$ . Below we present expressions for normally incident wave. The results for arbitrarily incident wave are obtained by the abovementioned replacements. We consider symmetric RSs It is in these structures that the total RT is possible in the absence of dissipation. Total RT means zero reflection coefficient. Partial RT may mean that there are frequencies at which a minimum of power reflection coefficient  $|R|^2$  is reached, which is nonzero even when there is no dissipation. Let us consider a five-layered symmetric RS. To calculate it, we may use the normalized transfer matrix of a layer

$$\hat{a}_n = \begin{bmatrix} \cos(k_0 t \sqrt{\varepsilon_n}) & i\tilde{\eta}_n^{-1} \sin(k_0 t \sqrt{\varepsilon_n}) \\ i\tilde{\eta}_n \sin(k_0 t \sqrt{\varepsilon_n}) & \cos(k_0 t \sqrt{\varepsilon_n}) \end{bmatrix}, \quad (2)$$

which involves the normalized wave admittances  $\tilde{\eta}_n$ , and the total five-layer RS transfer matrix. However, in dissipation-free RS it is convenient to use the transformation of wave admittances:

$$\tilde{y}_n^{in} = \tilde{y}_n \frac{\tilde{y}_{n+1}^{in} + i\tilde{y}_n \tan(k_0 t_n \sqrt{\varepsilon_n})}{\tilde{y}_n + \tilde{y}_{n+1}^{in} \tan(k_0 t_n \sqrt{\varepsilon_n})}. \quad (3)$$

Here  $\tilde{y}_n^{in}$  are the normalized admittances transformed to the planes of the layers and  $\tilde{y}_n$  are the normalized wave (medium) admittances of the layers. In the case of three identical plasma layers separated by two dielectric layers, we have a characteristic equation in the form (4) and (5):

$$\tilde{y}_{i3} = \frac{-\tilde{\eta} t_g t_h + i\tilde{\eta}^2(1 + it_g + t_h^2) + \tilde{\eta}^3 t_h(2 + it_g) + \tilde{\eta}^4 t_g t_h^2}{t_g t_h^2 - \tilde{\eta} t_h(2 + it_g) + i\tilde{\eta}^2(1 + it_g + t_h^2) + i\tilde{\eta}^3 t_g t_h}, \quad (4)$$

$$\tilde{y}_{i3} = \frac{it_g t_h + \tilde{\eta}(1 - t_g) + i\tilde{\eta}^2 t_h}{-t_h + \tilde{\eta}(1 - t_g) + \tilde{\eta}^2 t_h t_g}. \quad (5)$$

For simplicity, they are derived by transformation of the Eq. (3) type from two external boundaries to one internal. In these relations the following notations are used:  $t_g = \tan(k_0 t_\varepsilon \sqrt{\varepsilon})$ ,  $t_h = \tanh(k_0 t_d \sqrt{|\varepsilon_m|})$ ,  $\tilde{\eta} = \sqrt{|\varepsilon_m|/\varepsilon_d}$ ,  $t_\varepsilon$  and  $t_d$  being the thicknesses of the layers. The equation determines the complex resonance frequencies. At all other frequencies  $0 < |R|^2 < 1$ . Similar relations for symmetric structures can be obtained from the following considerations. A symmetric structure must have an odd number of layers  $N = 2M + 1$ ,  $n$  and  $N - n$ , layers and being similar,  $n = 1, 2, \dots, M = (N - 1)/2$ . This means that in the center of the layer with the number  $n = (N + 1)/2$  there is either magnetic or electric wall. Transforming the unit admittance  $\tilde{y}_{N+1} = 1$  of vacuum by means of Eq. (3) to the layer boundary and then to the layer center, we have as well as conditions,

$$\tilde{y}_{M+2}^{in} = \tilde{y}_{M+2} \frac{\tilde{y}_{M+3}^{in} + i\tilde{y}_{M+2} \tan(k_0 t_{M+2} \sqrt{\varepsilon_{M+2}})}{\tilde{y}_{M+2} + i\tilde{y}_{M+3}^{in} \tan(k_0 t_{M+2} \sqrt{\varepsilon_{M+2}})},$$

$$\tilde{y}^{in} = \tilde{y}_{M+1} \frac{\tilde{y}_{M+2}^{in} + i\tilde{y}_{M+1} \tan(k_0 t_{M+1} \sqrt{\varepsilon_{M+1}/2})}{\tilde{y}_{M+1} + i\tilde{y}_{M+2}^{in} \tan(k_0 t_{M+1} \sqrt{\varepsilon_{M+1}/2})},$$

as well as conditions

$$\tan(k_0 t_{M+1} \sqrt{\varepsilon_{M+1}}/2) = i(\tilde{y}_{M+2}^{in}/\tilde{y}_{M+1})^\nu,$$

where  $\nu = 1$  corresponds to a magnetic wall and  $\nu = -1$  to an electric wall. These are again implicit transcendent equations. It should be noted that when considering the wave incidence different from normal with the longitudinal components of the wave vectors  $k_{zn} = \sqrt{k_0^2 \varepsilon_n - k_x^2}$  and the transverse component  $k_x$ , the same equations describe plasmon polaritons moving along the  $x$ -axis in the multilayer structure [27].

## 2. Multilayer dielectric RS

Consider a dielectric plate with the thickness  $t_d$  and permittivity  $\varepsilon_d > 1$ . It is well known that such a plate is transparent at half-wave thickness  $t_d = \lambda \sqrt{\varepsilon_d}/2$ . The corresponding condition of zero reflection has the form,

$$\frac{1 + i\sqrt{\varepsilon} \tan(k_0 t_d \sqrt{\varepsilon_d})}{1 + i \tan(k_0 t_d \sqrt{\varepsilon})/\sqrt{\varepsilon_d}} = 1,$$

or  $\tan(k_0 t_d \sqrt{\varepsilon}) = 0$ , which yields the frequencies of transparency  $\omega_n = n\pi c/(t_d \sqrt{\varepsilon})$ ,  $n = 1, 2, \dots$ . If such a plate is overlaid on the left and on the right by two other identical plates with a different permittivity, then we obtain a RS, which is described by the same Eq. (1) taking into account the indicated correspondence. We will rewrite Eq. (1), denoting the parameters of the outer plates by index 1, and the inner plate by index 2. The transformation of the unit (normalized) vacuum admittance by the first plate yields

$$\tilde{y}_1 = \frac{1 + i\sqrt{\varepsilon_1} \tan(k_0 t_1 \sqrt{\varepsilon_1})}{1 + i \tan(k_0 t_1 \sqrt{\varepsilon_1})/\sqrt{\varepsilon_1}}. \quad (6)$$

The transformation by the second plate yields

$$\tilde{y}_2 = \frac{\tilde{y}_1 + i\sqrt{\varepsilon_2} \tan(k_0 t_2 \sqrt{\varepsilon_2})}{1 + i\tilde{y}_1 \tan(k_0 t_2 \sqrt{\varepsilon_2})/\sqrt{\varepsilon_2}}. \quad (7)$$

After the transformation by the third plate we get .

$$\tilde{y}_3 = \frac{\tilde{y}_2 + i\sqrt{\varepsilon} \tan(k_0 t_1 \sqrt{\varepsilon_1})}{1 + i\tilde{y}_2 \tan(k_0 t_1 \sqrt{\varepsilon_1})/\sqrt{\varepsilon_1}} = 1.$$

We set it equal to one to fulfil the condition of the absence of reflection. Therefore

$$\tilde{y}_2 = \frac{1 - i\sqrt{\varepsilon} \tan(k_0 t_1 \sqrt{\varepsilon_1})}{1 - i \tan(k_0 t_1 \sqrt{\varepsilon_1})/\sqrt{\varepsilon_1}}. \quad (8)$$

Comparing with Eq. (7), we find

$$\tilde{y}_1 = \frac{1 - i\sqrt{\varepsilon} \tan(k_0 t_1 \sqrt{\varepsilon_1}) - i\sqrt{\varepsilon_2} \tan(k_0 t_2 \sqrt{\varepsilon_2}) \times [1 - i \tan(k_0 t_1 \sqrt{\varepsilon_1})/\sqrt{\varepsilon_1}]}{1 - i \tan(k_0 t_1 \sqrt{\varepsilon_1})/\sqrt{\varepsilon_1} - [1 - i\sqrt{\varepsilon} \tan(k_0 t_1 \sqrt{\varepsilon_1})] \times [i \tan(k_0 t_2 \sqrt{\varepsilon_2})/\sqrt{\varepsilon_2}]}. \quad (9)$$

Finally, comparing with Eq. (6), we arrive at the desired characteristic equation. It is rather cumbersome, but can be simplified. For this purpose, it is necessary to convert  $\tan(k_0 t_2 \sqrt{\varepsilon_2})$  to the tangent of half the argument. We will not make calculations, but we will obtain two equations for the quantity  $x = \tan(k_0 t_2 \sqrt{\varepsilon_2}/2)$ , into which the resulting quadratic equation for  $x$  decomposes. Namely, the imposition of magnetic and electric walls at the center of the RS leads to the equations  $\tilde{y}_1 + ix\sqrt{\varepsilon_2} = 0$  and  $1 + i\tilde{y}_1 x/\sqrt{\varepsilon_2} = 0$ , i.e.  $x = i(\tilde{y}_1/\sqrt{\varepsilon_2})^{\pm 1}$ , where plus corresponds to the magnetic wall and minus to the electric one. The physical nature of the resonances obtained for and  $\varepsilon_1 \ll \varepsilon_2$  and  $\varepsilon_1 \gg \varepsilon_2$  is different, since the reflections of the partial waves with two directions inside the second plate upon their incidence on its boundaries are different. Particularly, they differ in phase. The case  $\varepsilon_1 \ll \varepsilon_2$  is close to the considered single plate, especially if  $t_1 \ll t_2$ . The case  $\varepsilon_1 = \varepsilon_2$  corresponds to a shift of the resonances to lower frequency compared to a single plate due to the actual path length increase by  $2t_1$ , and the case  $\varepsilon_1 \gg \varepsilon_2$  upon a certain ratio of the thicknesses can implement the mode of nearly standing waves with nodes at the boundaries of the plates. To obtain high-Q resonances, the permittivities of the layers should strongly differ. If we increase the number of layers to five, there will be a doublet instead of each resonance peak. A multilayer symmetric RS creates several frequency peaks. At large number of layers, these peaks transform into a transmission band of a corresponding photonic crystal. The RS operates like a bandpass filter with transmission bands and stop bands.

## 3. RS as a photonic crystal

It is possible to describe a RS with  $n$  periods  $d = t_1 + t_2$  with the transfer matrix  $\hat{a} = \hat{c}^n = (\hat{a}^{(1)}\hat{a}^{(2)})$ , where the transfer matrices for the layers are introduced. However, such matrix describes a structure with an even number of layers. For the RS the total matrix should be used  $\hat{b} = \hat{a}\hat{a}^{(1)}$ . Then the problem is solved in such a way:  $1 + R = b_{11}T + b_{12}T$ ,  $1 - R = b_{21}T + b_{22}T$ ,  $T = 2/(b_{11} + b_{12} + b_{21} + b_{22})$ , and for the normalized input wave admittance we get  $y_{in} = (1 - R)/(1 + R) = (b_{21} + b_{22})/(b_{11} + b_{12})$ . The characteristic equation has the form or  $y_{in} = 1$  or  $R = 0$ . Here all quantities are normalized. We have  $b_1 = a_{11}a_{11}^{(1)} + a_{12}a_{21}^{(1)}$  and analogous expressions for the rest elements of the total matrix. It is convenient to express the matrix elements  $\hat{a}$  of in terms of Chebyshev polynomials using recurrent formulae. Let us denote  $X = (c_{11} + c_{22})/2$ . Then the dispersion equation for the dispersion of a Bloch wave in an infinite photonic crystal (PC) takes the form

$$\cos(k_B d) = X. \quad (10)$$

For the first Brillouin zone  $-\pi < k_B d < \pi$  and  $-1 < X < 1$ . In the bandgap, the wave number

$k_B = i\kappa_B$  is imaginary, i.e.  $\cosh(\kappa_B d) - X > 1$ . At the band boundaries  $X = \pm 1$ . Resolving Eq. (10) in terms of arccosine or logarithm, we have  $\varphi_B = k_B d = \arccos(X) + 2n\pi$  or  $\varphi_B = k_B d = \pm i \ln(X - \sqrt{X^2 - 1}) + 2n\pi$ , i.e., the Bloch waves can be presented in the form  $\exp(\mp i k_B z)$ . Inside the PC the waves can be presented as

$$E_x = A^+ \exp(-i k_B z) + A^- \exp(i k_B z),$$

$$H_y = \sqrt{\varepsilon_0/\mu_0} k_B/k_0 [A^+ \exp(-i k_B z) - A^- \exp(i k_B z)].$$

These waves should be matched with the incident wave

$$E_x = \exp(-i k_0 z) + \operatorname{Re} x p(i k_0 z),$$

$$H_y = \sqrt{\varepsilon_0/\mu_0} [\exp(-i k_0 z) - \operatorname{Re} x p(i k_0 z)]$$

These waves should be matched with the incident wave, and with the transmitted wave  $E_x = T \exp(-i k_0(z-l))$ ,  $H_y = \sqrt{\varepsilon_0/\mu_0} T \exp(-i k_0(z-l))$ , where  $l$  is the total length of the structure. However, for a symmetric RS, the first layer should also be placed in front of it before the incident wave. This complicates the calculation. In addition, we must also solve Eq. (10) and determine dispersion  $k_B(k_0)$ . Such matching is reasonable in the case of a large number of periods. The transfer matrix method is more general and convenient. However, the determination of band boundaries based on Eq. (10) is convenient for synthesizing RSs with a given band. The PC-based description begins to work well at  $n \geq 40$ . The synthesis of a structure with given band can be performed based on the conditions  $X = \pm 1$ , and then using the transfer matrix algorithm to calculate the parameters  $R$  and  $T$  of the ultimate structure. If the losses can be really ignored, a better and faster method is to recalculate the wave admittances or impedances, since the transfer matrix method may be unstable. In this case, transparency  $D = |T|^2 = 1 - |R|^2$  can be determined through the reflection coefficient.

Another approximate possibility of analyzing the passage of photons through quasi-periodic layered structures, the photonic crystals, can be based on homogenization [28,29]. According to Rytov, homogenization in this case is quite simple, and it is possible both without taking into account spatial dispersion and with it [29]. Weak dissipation can lead to almost total transmission, while it strongly depends on the angle of incidence if the anisotropy axis of the metamaterial is rotated relative to the normal [29,30]. There are a number of misconceptions regarding the tunneling of photons through a PC regarding the time and rate of tunneling [23–25]. This is especially true for tunneling through band gaps, and not only in PCs. It was noted above that what propagates are quasi-particles — quasi-photons, determined by the collective interactions of photons and atoms. Their momentum may be imaginary. To determine the speed of movement and the time of tunneling, one cannot use interference measurements, which often show superluminal speeds. Strictly, the rate of such motion can be defined as the rate of energy transfer by a quasi-monochromatic wave [24,25].

#### 4. Permittivity dissipation and dispersion

Dissipation is related to the dispersion of permittivity, however, for purely dielectric RSs with highly transparent layers dispersion is usually weak, so that dissipation plays the main role. Below we demonstrate that a weak dissipation below 0.01 has practically no effect on the RT. Substantial reduction of RT is possible due to the dissipation above the level of 0.01. In metallic layers the frequency dispersion is very strong, and in the low-frequency region (below  $\omega_c$ ) a strong skin effect takes place with complex waves, strong dissipation and partial waves weakly changing in amplitude in the metallic layers as thick as a few nanometers. The main band-stop effect at low frequencies is due to reflection, and attenuation weakly contributes to the band-stop effect. In the plasmonic region ( $\omega_c \ll \omega < \omega_p$ ) the waves are evanescent and possess weak dissipation. In all cases the deceleration of waves strongly increases with a decrease in frequency and the penetration depth is always greater than 100 nm [31]. In a dissipative structure, there can be no total transmission (the number of photons is not conserved). Correspondingly, there is not total RT. This is the key distinction from the RT in quantum mechanics, where the number of particles is conserved. For RSs with transparencies close to unity, it is necessary to reduce losses in all possible ways. For metallic layers as thick as 10–20 nm and more, it is still possible to use the permittivity of a bulk metal sample. Except in the UV range, the permittivity of a metal is well described by the Drude–Lorentz formula, where the Lorentz term  $\varepsilon_L$  is constant and real:

$$\varepsilon_m = \varepsilon'_m - i\varepsilon''_m = \varepsilon_L - \omega_p^2/(\omega^2 - i\omega\omega_{0c}). \quad (11)$$

The quantity  $\varepsilon_L$  determines the short-wave, optical and UV properties of the metal, and in the range of our interest it is real and has the order of 10. We will determine the plasma frequency  $\omega_p$  in Eq. (1) from the concentration of charge carriers and the collision frequency  $\omega_{0c}$  and  $\varepsilon_L$  from the DC conductivity  $\sigma_0 = \varepsilon_0\omega_p^2/\omega_c$  and the condition of passing zero  $\varepsilon'_m$ . Considering resonance frequencies in the Lorentz term is important in the UV region, where one should take into account the electron interband transitions and the transitions between atomic energy levels. For our purposes, it is quite sufficient to take this term constant. So, for silver we can take  $\varepsilon_L = 9.3$ ,  $\omega_p = 1.57 \cdot 10^{16}$  Hz,  $\omega_{0c} = 3.56 \cdot 10^{13}$  Hz, and for copper  $\varepsilon_L = 13.09$ ,  $\omega_p = 1.65 \cdot 10^{16}$  Hz,  $\omega_{0c} = 5.41 \cdot 10^{13}$ . Here and in Eq. (1), the collision rates are presented for room temperature  $\tilde{T}_0 = 300$  K. In the case of an arbitrary temperature  $\tilde{T}$  for pure metals, there is a good correspondence between the dependence on temperature:  $\omega_c = \omega_{0c}\tilde{T}/\tilde{T}_0$ .

The results of calculating the absolute value of the transmission coefficient of quasi-periodic metal-dielectric structures with many periods are shown in Figs. 1. Results using homogenization are also presented there. As can be seen, they correspond well to a rigorous calculation. The

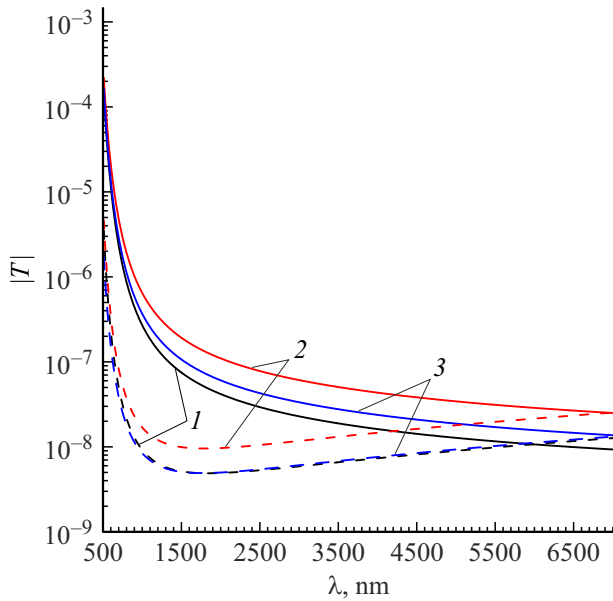
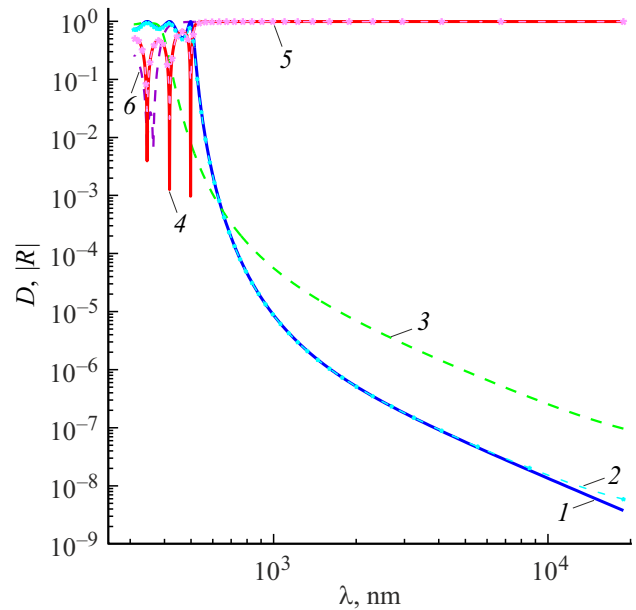


**Figure 1.** Absolute values of transmission coefficients as functions of wavelength based on homogenization (dashed curves) and on a rigorous model (solid curves) for a structure with  $t_m = t_d = 10$  nm, 22 periods, and a thickness of 440 nm. 1 — normal incidence, 2 — incidence of an  $E$  mode, 3 — incidence of an  $H$  mode (the incidence angle is  $\pi/4$ ).

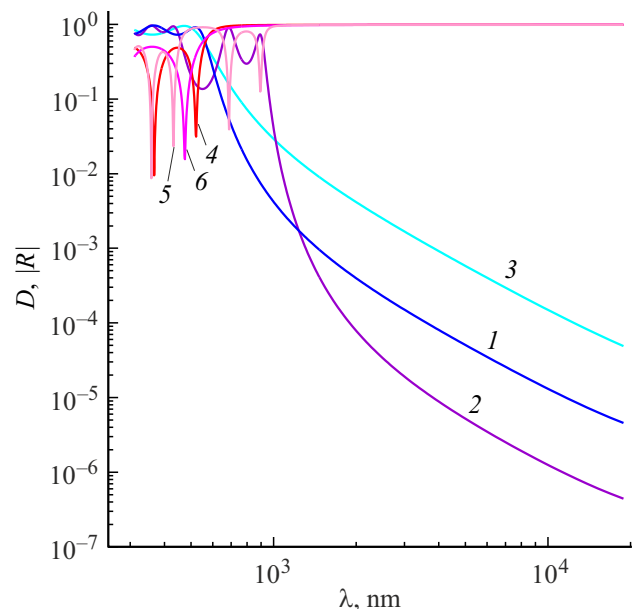
presented structure is transparent in the UV and short-wavelength part of the optical range. For transparency in the entire optical range, the number of periods should be reduced, and the thickness of the dielectric layers should be increased. Figure 2 presents the frequency characteristics of the transparency  $D = |T|^2$  and reflection coefficient absolute value  $|R|$  for a RS with two and three metallic layers separated by vacuum gaps. Curves 1 and 4 are presented for temperatures in 1 K. Curves 2 and 5 with symbols show the effect of room temperature. In the frequency range considered, for the used ratio  $\omega_{0c}/\omega_p \sim 0.001$  a decrease in temperature below the room one has practically no effect on the result. There is an expressed high-frequency region with numerous RT frequencies, which sharply transits to the region of strong screening in the IR range, when the transparency falls by a few orders of magnitude.

Figure 3 presents analogous results for an RS in the form of metallic layers separated by dielectric layers. No dielectric losses were taken into account. Figure 4 illustrates the calculation of dielectric RSs with and without the dielectric losses in them taken into account. The permittivity dispersion was not considered. Dielectric losses below  $\epsilon_d''/\epsilon_d' = 0.01$  practically do not affect the transmission. For simplicity, they were taken the same for all layers. Figure 5 demonstrates the effect of the incidence angle of  $p$ -polarized wave for a three-layered metal-dielectric RS. An increase in the incidence angle leads to a slight decrease in the band-stop effect in the IR region. The considered dependences on the incidence angle at fixed frequencies show resonances

that correspond to the excitation angles in the system of surface plasmon polaritons. In all cases in the optical range, the resonant behavior is strongly expressed, whereas in the IR range the transparency tends to zero with an increase in the wavelength. The Table shows the effect of dielectric losses on the complex resonance frequencies of an open



**Figure 2.** Dependences of  $D = |T|^2$  (curves 1-3) and  $|R|$  (4-6) on the wavelength (nm) for a tunnel RS with three 20 nm thick silver layers separated by vacuum gaps 150 (curves 1, 2, 4, 5) and 50 nm (3, 6). Curves 1, 4 are plotted for  $\bar{T} = 1$  K, the rest curves for  $\bar{T} = 300$  K.



**Figure 3.** Dependences of  $E = |T|^2$  (curves 1-3) and  $|R|$  (curves 4-6) on wavelength (nm) for tunnel RT at room temperature with three (1, 2, 4, 5) and two (3, 6) silver layers 10 nm thick separated by a dielectric  $\epsilon + d = 3$  with thicknesses 50 nm (1, 3, 4, 6) and 150 nm (2, 5).

Resonance frequencies  $\omega_n = \omega'_n + i\omega''_n$  (THz) and  $Q_n = \omega'_n/(2\omega''_n)$  factors for a five-layered dielectric RS, corresponding to the curves in Fig. 4

Number of resonance $n$	$\omega'_n$	$\omega''_n$	$Q_n$
$\varepsilon''_n/\varepsilon'_n = 0$			
1	3170.2	18.54	85.5
2	5850.4	17.08	171.3
$\varepsilon''_n/\varepsilon'_n = 0.01$			
1	3160.4	34.28	46.09
2	5848.3	46.31	63.14
$\varepsilon''_n/\varepsilon'_n = 0.1$			
1	3168.6	177.02	8.95
2	5835.1	308.73	9.45

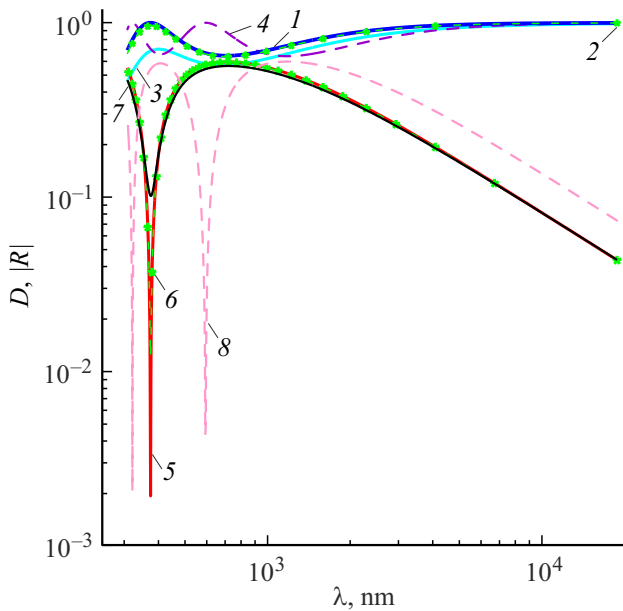


**Figure 4.** Transparency  $D$  (curves 1–4) and modulus  $|R|$  (5–8) for a three-layer dielectric RS (curves 1–3, 5–7) for  $t_1 = t_3 = 10$  nm,  $t_2 = 20$  nm,  $\varepsilon'_1 = \varepsilon'_3 = 9$ ,  $\varepsilon'_2 = 3$  and five-layer dielectric RS (4, 8) at  $t_1 = t_3 = t_5 = 10$  nm,  $t_2 = t_4 = 20$  nm,  $\varepsilon'_1 = \varepsilon'_3 = \varepsilon'_5 = 9$ ,  $\varepsilon'_2 = \varepsilon'_4 = 3$  and  $\varepsilon''_n/\varepsilon'_n = 0$  (curves 1, 4, 5, 8),  $\varepsilon''_n/\varepsilon'_n = 0.01$  (2, 6),  $\varepsilon''_n/\varepsilon'_n = 0.1$  (3, 7).

five-layered dielectric resonator. The losses substantially reduce the Q factor, if  $1/Q$  is comparable with them. If the losses are still greater, the RT virtually vanishes.

The high intrinsic Q factor is inversely proportional to the spectral linewidth and is associated with a long energy level lifetime. In other words, to establish such oscillations in the case of excitation, a long time is needed, substantially exceeding  $2\pi/\omega_0$ . A photon is defined by a monochromatic wave, for which the transit time is not defined. Such a wave

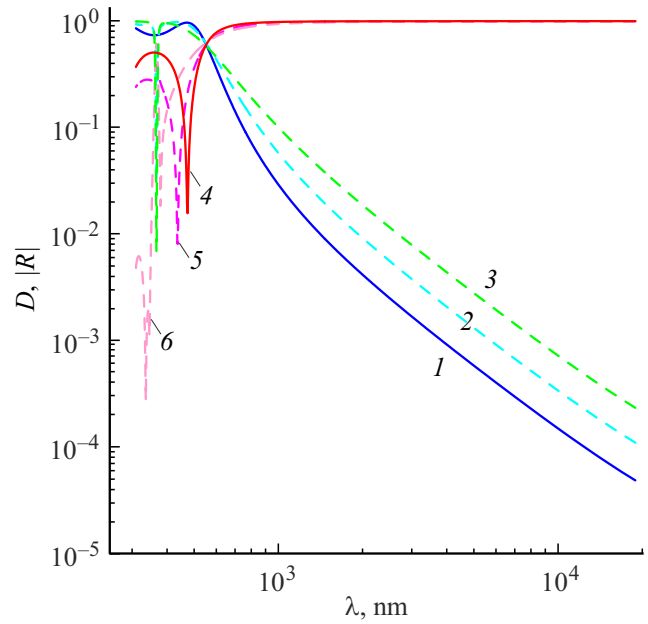


**Figure 5.** Dependence of the transparency of  $D$  (curves 1–3) and  $|R|$  (2–6) on the wavelength (nm) for a three-layer tunnel RS with two silver layers  $t_m = 10$  nm and a dielectric layer  $\varepsilon_d = 3$ ,  $t_d = 50$  nm at different angles of incidence: 0 (curves 1, 4),  $\pi/4$  (2, 5),  $\pi/3$  (3, 6).

is a stream of photons with the same energy  $\hbar\omega_0$ , where the localization of each is not defined. Only the energy density per unit volume and, accordingly, the density of the photon flux can be introduced. For a quasi-monochromatic wave with a narrow spectrum  $\Delta\omega = |\omega - \omega_0| \ll \omega_0$ , containing mainly photons with the frequencies close to  $\omega_0$ , it is possible to speak about approximate transit time of photons with the frequency  $\omega_0$  through the RS. Rigorously, the duration of wave packet tunneling is determined by the energy transfer with averaging over the spectrum [23]. Obviously, the result for photons with the given frequency will be the more accurate, the narrower the spectrum. Clearly, the tunneling time cannot be shorter than the lifetime of the resonant energy level, i.e., the time required for establishing the oscillation in the structure. This is also true for the tunneling through the allowed bands of PC. These bands should form due to multiple reflections, which takes certain time. Such behavior is demonstrated by, e.g., the finite difference time domain (FDTD) electrodynamic modeling packages: a rather weak (precursor) signal at the output of RS with the length  $d$  appears in time after the approach of the wave packet front edge  $\tau = d/c$ , and then after a large enough transient time the signal becomes amplified and nearly harmonic. Upon tunneling through a bandgap, the signal appeared after the time  $\tau$  is begins to be gradually suppressed. This again testifies that the tunneling of photons is a collective multiphoton effect of their interaction with matter.

## 5. Using tunneling RSs for IR screening of window panes

Window glasses are currently subject to very high requirements of a different nature [32]. One of the most important requirements is the property not to transmit infrared radiation and to transmit the entire visible range. This is due to the fact that the walls of buildings practically do not transmit infrared radiation, but window panes transmit it very well. At room temperature  $T_0$  about 300 K, thermal radiation inside a building can with good approximation considered equilibrium Planck radiation, i.e. equivalent to the ideal blackbody radiation. If the room temperature is  $\tilde{T}_0 = 27^\circ\text{C}$  and the temperature outside is  $\tilde{T} = -23^\circ\text{C}$ , then for the temperature difference of  $50^\circ$  the heat flux through the windows from the building is rather high (394 W from a square meter without taking into account the small absorption in the glass). If in summer the outside temperature is  $\tilde{T} = 37^\circ\text{C}$ , then the temperature difference will be ten degrees and the corresponding flux is also essential. The maximum density of thermal radiation is  $u_p = \hbar\omega^3 f_{FD}(\omega, \tilde{T})/(\pi^2 c^3)$ , where  $f_{FD}(\omega, \tilde{T}) = [\exp(\hbar\omega/(k_B\tilde{T})) - 1]^{-1}$  is the Bose–Einstein function. If the area of the windows is  $S$ , then the energy flux per second through almost transparent window glasses equals  $P = \sigma_{SB}((\tilde{T})^4 - T_0^4)W$ . Here is the Stefan–Boltzmann constant. Here  $\sigma_{SB}$  is the Stefan–Boltzmann constant. The flux maximum at temperatures  $300 \pm 500\text{ K}$  lies in the wavelength range from  $8.27\ \mu\text{m}$  to  $11.59\ \mu\text{m}$ , i.e. in the middle of the IR range. Therefore, the problem is to screen the IR range with the maximum screening at wavelengths about  $10\ \mu\text{m}$ , keeping the transmission high enough in the visible range. The use of only dielectric layers in this case is not efficient, since ensuring the resonant transmission at short optical wavelengths we will not achieve band-stop effect of long IR waves. Metals reflect electromagnetic radiation well. In optics, thin layers of metal as thick as a few nm are semitransparent. There are many publications on layered photonic structures (see, e.g., [33–35] and references therein). However, there are few publications on RT of photons in metal-dielectric structures. Refs. [36,37] consider multilayer screens with such films and alternating dielectric layers, e.g., made of  $\text{SiO}_2$ . They can be fabricated on glass with a thickness of several mm. Then the problem is to synthesize the optimal structure of such a coating on glass. In this case, strong suppression of IR radiation is possible while maintaining good transparency in the optical range [36,37]. In the microwave range, as the wavelength increases, transparency also improves, which, for example, is important for cellular communications. However, technologically it is difficult and expensive to make such a multilayer coating. Window glass with a thickness of several millimeters can be symmetrically coated with RS on both sides. Another way is to cover one side of the glass and then cover it with another glass of the same type,

i.e. perform an RS in the center of the double pane. This is a more expensive technology. It is cheaper, but less efficient, to perform non-symmetrical coatings. The cheapest way is to introduce metal nanoparticles into glass to a certain depth (see, e.g., [32]). It can be done by introducing nanoparticles into the glass melt and depositing a thin layer of the melt on the base glass. In this way, several layers can be fabricated hundreds of nanometers thick. The effective permittivity of such layers can be estimated using the Bruggeman formula (see [29]), or based on the simple homogenization formula  $\varepsilon_{\perp}^{ef} = c_m\varepsilon_m + (1-c_m)\varepsilon_d$ . Here  $c_m$  is the concentration of metallic particles. For layered structures, this formula is more accurate than Bruggeman's one. It corresponds to the fact that the depth of penetration into the metal is much smaller than the size of the nanoparticles, i.e. the field inside them is uniform and has a dipole character [31]. Accordingly, for the polarization of particles, we can write  $\mathbf{P}_m = c_m\varepsilon_0(\varepsilon_m - \varepsilon_d)\mathbf{E}$ . Taking into account that  $\mathbf{P} = \mathbf{P}_m + \mathbf{P}_d$ ,  $\mathbf{P}_d = (1 - c_m)\varepsilon_0\varepsilon_d\mathbf{E}$ , we get the above relation. Note that the Bruggeman formula corresponds to the above one for planar layers after introducing depolarization coefficients (factors) into it. Such a multiphase formula has the form

$$\sum_{j=1}^n c_j \frac{\varepsilon_{\alpha}^{ef} - \varepsilon_j}{\varepsilon_{\alpha}^{ef} + L_{\alpha}(\varepsilon_j - \varepsilon_{\alpha}^{ef})} = 0, \quad \alpha = x, y, z. \quad (12)$$

For planar layers  $L_x = L_y = 0$ ,  $L_z = 1$ , we immediately get Rytov's homogenization [28,29]:  $\varepsilon_{\perp}^{ef} = c_1\varepsilon_1 + c_2\varepsilon_2$ . By introducing metal cylindrical particles with magnetic properties in the presence of magnetic fields in the glass, it is possible to control their orientation along the field when the glass layer is solidified and to create optically anisotropic structures. They transmit better in the direction of particle alignment, i.e., not upon the normal incidence, but when the anisotropy axis is rotated with respect to the normal and the wave is incident along this axis [29,30]. The effect of somewhat of jalousie arises. In this case, the tensor of effective permittivity can be obtained based on Eq. (12) using a rotation matrix [30]. Note that the Garnett formula is not applicable for metal particles [38]. It leads to resonances of the localized plasmon type in the frequency region, where  $\varepsilon_m = -2\varepsilon_d$ , i.e., at frequencies  $\omega \approx \omega_p/\sqrt{\varepsilon_L + 2\varepsilon_d}$ . In this case,  $\varepsilon^{ef}$  changes the sign. Figure 4 presents the comparison of results obtained using Eq. (12) for spherical particles and for layers with the results obtained using the above formula for  $\varepsilon_{\perp}^{ef}$ . The negative real part of permittivity follows from Bruggeman formula upon exceeding the percolation threshold, i.e., a strong saturation of glass with metallic particles is necessary. In reality, this is an overstated requirement. Note also that the Bruggeman formula works worse in the vicinity of the percolation threshold and should be used at high concentration  $c_m > 1/2$ . A usual 4 mm-thick window glass is 12600 wavelengths thick for a medium-wavelength, say, green light. This means that the power reflection  $|R|^2$  in the optical range rapidly changes from zero to 0.07 within a small frequency region, i.e., there are many frequencies of total tunneling. They are also many

in the IR range, but they are sparser. In this range, the losses in the glass should be taken into account. The RS implementation on a glass leads to the superposition of such minor oscillations on strongly expressed resonances with substantial band-stop effect in the IR range. We did not take into account dispersion and glass losses in the IR range. Compared to the effect of metallic RS, this is a weak effect. Near IR (NIR) and short-wave IR (SWIR) radiation are well transmitted through a usual window glass. The medium wave IR radiation is absorbed stronger. In principle, these effects can be taken into account, but their contribution is minor.

## Conclusion

The structures that almost totally transmit photons with certain frequencies, i.e., implement RT, are considered. The total RT is related to negligibly small losses, which can be reached in at ultralow temperatures. The RT is due to complex resonance eigenfrequencies and it is the closer to total tunneling, the higher is the Q factor of the open resonator, corresponding to the RS. For simplest RSs, we present the characteristic equations that determine such frequencies. Their derivation is analogous to the determination of dispersion for surface plasmon polaritons in the structure and requires the iterative solution of characteristic equation. It is interesting to note that in both case the condition for the existence of solutions is zero reflection coefficient. The difference is that in the first case we find complex frequencies from given real wave vector components of the incident wave, whereas in the second case we find complex values of the wave vector in vacuum from given real frequencies. These complex values of the vacuum wave vector determine the wave type: it can be an inflowing surface or outflowing (anti-surface) wave [39,40]. Upon the frequency change, a transition from one type of the wave to another is possible. In the case of inflowing wave, the energy is transferred from vacuum to the structure and absorbed. In the case of outflowing wave, the accumulated energy is radiated into vacuum, therefore, the wave decays in the longitudinal direction even in the absence of dissipation. The frequency of the transition determines the surface wave cutoff and corresponds to propagation with the speed of light. It is interesting to note that for a loss-free semispace this condition corresponds to the Brewster condition [39]. We considered the simplest case of normal incidence. In the case of  $E$  or  $H$  waves ( $p$  polarization or  $s$  polarization) the difference is only in the change of wave impedances of admittances, which will include the vector components tangent to interfaces. An increase in the number of layers leads to an increase in the number of resonant transmission peaks, i.e., to the formation of a transmission band. In this way, the transition to a photonic crystal structure is implemented. In RSs with a large number of periods, the calculation methods based on homogenization are considered. It should also be noted

that Hartmann's paradox [41] does not hold in the structures under consideration [23–25].

The application of RSs is demonstrated by an example of window glass screening, which allows reducing the transmission of thermal radiation by several orders of magnitude, while in the visible range the RT is achieved. Manufacturing of the appropriate coatings by implanting metallic particles into glass layers and determining the effective permittivity of such layers are considered. Under the action of waves incident at various angles, the excitation of surface plasmons is possible in the coatings considered. This means that when considering these surfaces at different angles in the reflected light in the optical and IR ranges, glares of different colors (frequencies) that change when changing the angles should be observed.

## Acknowledgments

The work was supported by the Ministry of Science and Higher Education of the Russian Federation within the frameworks of the State Assignment (project № FSRR-2023-0008).

## Conflict of interest

The author declares that he has no conflict of interest.

## References

- [1] R. Tsu, L. Esaki. *Appl. Phys. Lett.*, **22**(11), 562 (1973). DOI: 10.1063/1.1654509
- [2] L.L. Chang, L. Esaki, R. Tsu. *Appl. Phys. Lett.*, **24**, 593 (1974). DOI: 10.1063/1.1655067
- [3] L. Esaki. *J. Quantum Electron.*, **QE-22**(9), 1611(1986). DOI: 10.1007/978-94-009-3073-5\_4
- [4] Y. Arakawa, A. Yariv. *J. Quantum Electron.*, **QE-22**(9), 1887 (1986). DOI: 10.1109/JQE.1986.1073185
- [5] E.X. Ping, H.X. Jiang. *Phys. Rev. B*, **40**(17), 11792 (1989). DOI: 10.1103/PhysRevB.40.11792
- [6] M.V. Davidovich. *JETP Lett.*, **110**, 472 (2019). DOI: 10.1134/S0370274X19190068
- [7] M.V. Davidovich, I.S. Nefedov, O.E. Glukhova, M.M. Slepchenkov. *J. Appl. Phys.*, **130**, 204301(1–11) (2021). DOI: 10.1063/5.0067763
- [8] L.D. Macks, S.A. Brown, R.G. Clark, R.P. Starrett, M.A. Reed, M.R. Deshpande, C.J.L. Fernando, W.R. Frensley. *Phys. Rev. B*, **54**(7), 4857 (1996). DOI: 10.1103/PhysRevB.54.4857
- [9] J.M. Xu, V.V. Malov, L.V. Iogansen. *Phys. Rev. B*, **47**(12), 7253 (1993). DOI: <https://doi.org/10.1103/PhysRevB.47.7253>
- [10] V.F. Elesin. *JETP*, **101**, 795 (2005). DOI: 10.1134/1.2149060
- [11] V.F. Elesin. *JETP*, **89**, 377 (1999). DOI: 10.1134/1.558994
- [12] V.F. Elesin. *JETP*, **92**, 710 (2001). DOI: 10.1134/1.1371352
- [13] V.F. Elesin. *JETP*, **94**, 794 (2002). DOI: 10.1134/1.1477905
- [14] V.F. Elesin. *JETP*, **117**, 950 (2013). DOI: 10.1134/S1063776113130104
- [15] V.F. Elesin. *JETP*, **118**, 951 (2014). DOI: 10.1134/S1063776114060041
- [16] O. Pinaud. *Appl. Phys.*, **92**(4), 1987 (2002). <https://doi.org/10.1063/1.1494127>

- [17] I.I. Abramov, I.A. Goncharenko, N.V. Kolomejtseva. *Semiconductors*, **39** (9), 1102 (2005). DOI: 10.1134/1.2042607
- [18] V.N. Mantsevich, N.S. Maslova, P.I. Arseyev. *Solid State Comm.*, **152** (16), 1545 (2012). DOI: 10.1016/j.ssc.2012.05.027
- [19] L.V. Iogansen. *Soviet Phys. JETP*, **18** (1), 146 (1964).
- [20] D.J. Day, Y. Chung, C. Webb, J.N. Eckstein, J.M. Xu, M. Sweeny. *Appl. Phys. Lett.*, **57** (12), 1260 (1990). DOI: 10.1063/1.103503
- [21] T.C.L.G. Sollner, W.D. Goodhue, P.E. Tannenwald, C.D. Parker, D.D. Peck. *Appl. Phys. Lett.*, **43** (6), 588 (1983). DOI: 10.1063/1.94434
- [22] E.A. Nelin. *Phys. Usp.*, **50** (3), 293 (2007). DOI: 10.1070/PU2007v050n03ABEH006091
- [23] M.V. Davidovich. *JETP*, **130**, 35 (2020). DOI: 10.1134/S1063776119120161
- [24] M.V. Davidovich. *J. Samara State Tech. Univer. Ser. Phys. Mathemat. Sci.*, **24** (1), 22 (2020).
- [25] M.V. Davidovich. *Izvestiya of Saratov Univer. New Series. Series: Physics*, **21** (2), 116 (2021). DOI: 10.18500/1817-3020-2021-21-2-116-132
- [26] A. Alú, M.G. Silveirinha, A. Salandrino, N. Engheta. *Phys. Rev. B*, **75**, 155410(1–13) (2007). DOI: 10.1103/PhysRevB.75.155410
- [27] M.V. Davidovich. *Quant. Electron.*, **47** (6), 567 (2017). DOI: 10.1070/QEL16272
- [28] S.M. Rytov. *Sov. Phys. JETP*, **2** (3), 466 (1956).
- [29] M.V. Davidovich. *Phys. Usp.*, **62**, 1173 (2019). DOI: 10.3367/UFNe.2019.08.038643
- [30] M.V. Davidovich. *Comp. Optics*, **45** (1), 48 (2021). DOI: 10.18287/2412-6179-CO-673
- [31] M.V. Davidovich. DOI: 10.1134/S106378422207012X
- [32] V.A. Maiorov. *Opt. Spectr.*, **124** (4), 594 (2018). DOI: 10.1134/S0030400X18040112
- [33] A.M. Merzlikin. *Mezoskopicheskiye efekty kogerentnogo rasprostraneniya i lokalizatsii polyarizovannykh elektromagnitnykh voln v fotonnykh kristallakh i neuporyadochennykh sloistykh sredakh*. (Diss. d.f.-m.n. M., 2016 (in Russian)).
- [34] L.I. Deych, A. Yamilov, A.A. Lisyans. *Phys. Rev. B*, **64**, 075321(1–13) (2001). DOI: 10.1103/PhysRevB.64.075321
- [35] D.S. Citrin, W. Harshawardhan. *Phys. Rev. B*, **60** (3), 1759 (1999). DOI: 10.1103/PhysRevB.60.1759
- [36] M.V. Davidovich, R.K. Yafarov, D.M. Doronin, P.A. Shilovskiy. *Fizika volnovykh protsessov i radiotekhnicheskiye sistemy*, **2** (19), 2012 (2008) (in Russian).
- [37] M.V. Davidovich, I.A. Kornev. *Comp. Opt.*, **43** (5), 765 (2019). DOI: 10.18287/2412-6179-2019-43-5-765-772
- [38] B.A. Belyaev, V.V. Tyurnev. *JETP*, **127**, 608 (2018). DOI: 10.1134/S1063776118100114
- [39] L.A. Vainshtein. *Elektromagnitnye volny* (Radio i Svyaz<sup>2</sup>, Moscow, 1988) (in Russian).
- [40] M.V. Davidovich. *J. Comm. Technol. Electron.* **63**, 497 (2018). DOI: 10.1134/S1064226918060050
- [41] A.B. Shvartsburg. *Phys. Usp.*, **50**, 37 (2007). DOI: 10.1070/PU2007v050n01ABEH006148

*Translated by Ego Translating*